

The fractional parentage expansions given here have been obtained for the purpose of using them for calculations of two-particle interactions in nuclei. They can also be applied in atomic spectroscopy (after the replacements  $j_i \rightarrow \ell_i$ ,  $J \rightarrow L$ ,  $T \rightarrow S$ ).

<sup>1</sup>G. Racah, Phys. Rev. **62**, 438 (1942).

<sup>2</sup>G. Racah, Phys. Rev. **63**, 367 (1943).

<sup>3</sup>M. G. Redlich, Phys. Rev. **99**, 1427 (1955).

<sup>4</sup>C. Schwartz and A. de-Shalit, Phys. Rev. **94**, 1257 (1954).

<sup>5</sup>H. A. Jahn, Phys. Rev. **96**, 989 (1954).

<sup>6</sup>M. J. Englefield, Phys. Rev. **98**, 1213 (1955).

<sup>7</sup>H. A. Jahn and J. Hope, Phys. Rev. **93**, 318 (1954).

<sup>8</sup>A. de-Shalit, Phys. Rev. **91**, 1479 (1953).

<sup>9</sup>A. R. Edmonds, Angular Momentum in Quantum Mechanics, CERN 55-26, Geneva, 1955.

Translated by W. H. Furry  
131

SOVIET PHYSICS JETP

VOLUME 34 (7), NUMBER 3

SEPTEMBER, 1958

### ON THE THEORY OF PHOTONUCLEAR REACTIONS

V. M. AGRANOVICH and V. S. STAVINSKII

Submitted to JETP editor September 30, 1957

J. Exptl. Theoret. Phys. (U.S.S.R.) **34**, 700-706 (March, 1958)

The cross section is computed for the capture of gamma rays by nuclear matter at giant resonance energies.

IN theoretical investigations of giant resonance in photonuclear reactions, extensive use has been made of two models for interactions between gamma rays and nuclei. Migdal,<sup>1</sup> Goldhaber and Teller<sup>2</sup> and others regarded giant resonance as the result of an interaction between gamma rays and the collective dipole vibrations of nuclei. In contrast with this collective aspect, Wilkinson<sup>3</sup> and Burkhardt<sup>4</sup> have used the shell model in a detailed study of the mechanism of gamma-ray capture as the result of the excitation of single nucleons. However, neither model provides an explanation of all of the experimental data. For example, recent calculations based on the collective model<sup>5</sup> give a width of giant resonance in  $(\gamma, n)$  reactions which is much smaller than the observed width. On the other hand, the shell model gives incorrect frequencies for giant resonance.<sup>4\*</sup> The principal defect of the calculations that have been mentioned is apparently the use of incorrect wave

functions to describe highly excited nuclear states.

It is shown in several papers<sup>6-9</sup> that experiments on slow neutron scattering by medium and heavy nuclei can be interpreted satisfactorily if in constructing wave functions for highly excited states account is taken of the possibility that the excitation energy of a single particle is redistributed among other degrees of freedom. In our calculation of the photonuclear absorption cross section we shall use herein the method of Lane, Thomas, and Wigner<sup>7</sup> for constructing the wave functions of excited states, taking the above mentioned possibility into account.

#### 1. CALCULATION OF THE PHOTONUCLEAR ABSORPTION CROSS SECTION

The nonrelativistic operator for the interaction between an electromagnetic field and a system of nucleons is

$$H' = - \sum_n \left[ \left( \frac{e}{Mc} \right) pA \left( \frac{1}{2} - t_{zn} \right) + \left\{ \mu_p \left( \frac{1}{2} - t_{zn} \right) + \mu_n \left( \frac{1}{2} + t_{zn} \right) \right\} \sigma \nabla \times \underline{A} \right]. \quad (1)$$

If  $\Psi_0$  and  $\Psi_{E\gamma}$  are the wave functions of the nu-

\*Note added in proof. The computed giant-resonance frequencies are close to the observed frequencies when the effective nucleon mass is set equal to half of the true mass for all excitation energies,<sup>10</sup> but there is no other basis for this assumption.

cleonic system that represent the ground level and an excited level which is higher by the energy of the absorbed gamma ray, the gamma-ray absorption probability per second<sup>10</sup> is

$$P = \frac{2\pi}{\hbar} |H'_{0,E_\gamma}| \rho(E_\gamma), \quad (2)$$

where  $\rho(E_\gamma)$  is the density of levels with excitation energy  $E_\gamma$  and

$$H'_{0,E_\gamma} = \int \Psi_0^* H' \Psi_{E_\gamma} d\tau. \quad (3)$$

For the sake of simplicity we shall consider a system of  $A$  nucleons in a sufficiently large volume  $V$ . In the self-consistent field model the ground level of this system is represented by a completely filled Fermi sphere with the maximum wave number  $k_F$ . The self-consistent potential which corresponds to an excited level of the system differs from the self-consistent potential for the ground level. For this reason, and also because of the strong correlation between nucleons in a nucleus, the wave function  $\Psi_{E_\gamma}$  can be represented as follows:

$$\Psi_{E_\gamma} = \sum_b C_b \Phi_b, \quad (4)$$

where  $\{\Phi_b\}$  denotes different Slater determinants composed of single-particle wave functions that represent the motion of single nucleons in a constant potential which is self-consistent for the ground state of the nucleus.\* Following Ref. 7, it is assumed that the principal contributions to Eq. (4) come from states  $\Phi_b$  which represent energies  $\epsilon_b$  in a range of width  $W$  around  $E_\gamma$ . The width  $W$ , which is defined by

$$W^2 = \sum_b (E_\gamma - \epsilon_b)^2 |C_b|^2, \quad (5)$$

is directly related to the imaginary part of the optical potential.<sup>7-9</sup> We shall also assume that it is sufficient to limit ourselves in (4) to states  $\Phi_b$  which represent the emergence of only a single nucleon above the Fermi surface.

Using (4), (3), and (2), we find

$$P = \frac{2\pi}{\hbar} \rho(E_\gamma) \sum_b |C_b|^2 |M_{b0}|^2, \quad (6)$$

where

$$M_{b0} = \int \Phi_b^* H' \Phi_0 d\tau. \quad (7)$$

In (6), following Refs. 7 and 11, we have omitted

\*In the approximation used below  $\Psi_0 = \Phi_0$ .

the interference terms containing the products  $C_b C_b^*$ . Going from a sum to an integral in (6), we obtain

$$P = \frac{2\pi}{\hbar} \rho(E_\gamma) \int_0^\infty |C_b|^2 \rho(\epsilon_b) |\overline{M_{b0}}|^2 d\epsilon_b. \quad (8)$$

In (8)  $|\overline{M_{b0}}|^2$  is the square of the absolute value of the transition matrix element averaged over all levels of energy  $\epsilon_b$ . From the normalization of  $\Psi_{E_\gamma}$  it follows that

$$\int_0^\infty |C_b|^2 \rho(\epsilon_b) d\epsilon_b = 1. \quad (9)$$

Using the assumption of Ref. 7 that the principal contributions to (4) come from the states  $\Phi_b$  with energy  $\epsilon_b$  close to  $E_\gamma$  within a range of width  $W$ , as was done in Ref. 8, we put

$$|C_b|^2 \rho(\epsilon_b) = \frac{B(E_\gamma)}{\Omega} \exp\{- (E_\gamma - \epsilon_b)^2 / \Omega^2\}. \quad (10)$$

In (10), which satisfies (9),

$$B(E_\gamma) = \frac{2}{V\pi} [1 + \Phi(x)]^{-1}, \quad (11)$$

where

$$x = E_\gamma / \Omega, \quad \Phi(x) = \frac{2}{V\pi} \int_0^x e^{-t^2} dt.$$

The function  $\Omega \equiv \Omega(E_\gamma)$  in the approximation represented by (10) is, in virtue of (5), related to  $W(E_\gamma)$  as follows:

$$W^2(E_\gamma) = \frac{\Omega^2(E_\gamma)}{2[1 + \Phi(x)]} \left\{ 1 + \Phi(x) - \frac{2x}{V\pi} e^{-x^2} \right\}. \quad (12)$$

In calculating the matrix element (7) we neglect the interaction of the electromagnetic field with the nucleonic magnetic moments. In this approximation

$$|M_{0b}|^2 = \frac{Z^2 e^2 \hbar^2}{M^2 c^2} (\mathbf{A}_0 \mathbf{k}_1)^2 \delta_{\mathbf{k}_2, \mathbf{k}_1 + \mathbf{Q}}. \quad (13)$$

Here  $\mathbf{k}_1$  and  $\mathbf{k}_2$  are wave vectors that represent a hole inside the Fermi sphere and a nucleon outside. These wave vectors are related\* as follows ( $|\mathbf{k}_2| > k_F > |\mathbf{k}_1|$ ):

$$\hbar^2 k_2^2 / 2M^* - \hbar^2 k_1^2 / 2M^* = \epsilon_b. \quad (14)$$

In deriving (13) the vector potential was assumed to have the form

$$\mathbf{A} = \mathbf{A}_0 \exp\left\{ i \frac{E_\gamma t}{\hbar} + i \mathbf{Q} \mathbf{r} \right\}. \quad (15)$$

\*Here  $M^*$  is the effective mass of a nucleon in the nucleus.

By definition,

$$\overline{|M_{0b}|^2}_{\epsilon_b} = \sum_{b, \epsilon = \epsilon_b} |M_{0b}|^2 / g_{\epsilon_b}, \quad (16)$$

where  $g_{\epsilon_b}$  is the number of states  $\Phi_b$  with excitation energy  $\epsilon_b$ . It follows from (13) and (14) that not all levels with  $\epsilon_b$  give a non-vanishing matrix element  $M_{0b}$ . It also follows from these equations that when (14) is fulfilled  $M_{0b} \neq 0$  when\*

$$k_{1z} = M^* \epsilon_b / \hbar^2 Q - Q / 2 \equiv k_0. \quad (17)$$

Also, from the condition  $k_0^2 \leq k_F^2$  it follows that  $M_{0b}$  can be non-vanishing only for values of  $\epsilon_b$  within the limits

$$0 < \epsilon_b < \frac{\hbar^2 Q}{M^*} \left( k_F + \frac{Q}{2} \right) \equiv \epsilon'. \quad (18)$$

For a fixed value of  $\epsilon_b$  the range of variation of  $k_1$  is bounded by

$$k_F^2 \geq k_1^2 \geq k_F^2 - 2M^* \epsilon_b / \hbar^2 \equiv k_{\min}^2, \quad (19)$$

which follows from (14) and the Pauli principle ( $k_2^2 > k_F^2$ ). From (17) and (19) we find that the end of the vector  $k_1$ , for states  $\Phi_b$  ( $k_2 = k_1 + Q$ ) which give a non-vanishing matrix element  $M_{0b}$ , lies within a circular ring  $S$  in the plane  $k_{1z} = k_0$ . The radii of the ring are

$$\rho_{\max} = \sqrt{k_F^2 - k_0^2}, \quad (20)$$

$$\rho_{\min} = \begin{cases} \sqrt{k_F^2 - 2M^* \epsilon_b / \hbar^2 - k_0^2}, & \text{for } 0 < \epsilon_b < \epsilon'', \\ 0 & \text{for } \epsilon'' < \epsilon_b < \epsilon', \end{cases}$$

where

$$\epsilon'' = \frac{\hbar^2 Q}{M^*} \left( k_F - \frac{Q}{2} \right). \quad (21)$$

Therefore†

$$\sum_{b, \epsilon = \epsilon_b} |M_{0b}|^2 = \frac{Z^2 e^2 \hbar^2}{M^2 c^2} |A_0|^2 \sum_S k_{1x}^2$$

$$= \frac{Z^2 e^2 \hbar^2 |A_0|^2}{M^2 c^2} \frac{V^{1/2}}{(2\pi)^2} \frac{1}{4} (\rho_{\max}^4 - \rho_{\min}^4). \quad (22)$$

In computing the total number of states with energy  $\epsilon_b$  it must be kept in mind that (14) is the only limitation on the magnitude of  $k_2$ . Therefore

$$g_{\epsilon_b} = \frac{V^{1/2}}{(2\pi)^3} (4\pi)^2 \left\{ \frac{k_F^5 - k_{\min}^5}{5} + \frac{2M^* \epsilon_b}{\hbar^2} \frac{k_F^3 - k_{\min}^3}{3} \right\}. \quad (23)$$

Thus, from (16), (22), and (23) we obtain

$$\overline{|M_{0b}|^2} = \left( \frac{Ze\hbar |A_0|}{Mc} \right)^2$$

$$\times \frac{5\pi^2}{8V} \frac{(\rho_{\max}^4 - \rho_{\min}^4)}{k_F^5 - k_{\min}^5 + (10M^* \epsilon_b / 3\hbar^2)(k_F^3 - k_{\min}^3)}. \quad (24)$$

Substituting (10) and (24) into (8) and integrating, we obtain

$$P = \left( \frac{Ze\hbar |A_0|}{Mc} \right)^2 \frac{\pi^3 (M^* c / \hbar k_F)^2}{V \hbar k_F} \varphi_2(x) \rho(E_\gamma), \quad (25)$$

where

$$\varphi_2(x) = \frac{1}{1 + \Phi(x)} \left\{ \left[ \left( \frac{\hbar k_F}{M^* c} \right)^2 - 1 - x^2 \left( \frac{2M^* \Omega}{\hbar^2 k_F^2} \right)^2 \frac{1}{16} \left( \frac{\hbar k_F}{M^* c} \right)^4 \right] \right.$$

$$\times [\Phi(x) - \Phi(\gamma x)] + \frac{V^2}{x} [(2 - \gamma) \Phi_1(x\gamma\sqrt{2}) - \Phi_1(x\sqrt{2})]$$

$$\left. - \frac{1}{2x^2} [\Phi(x) - \Phi(\gamma x)] \right\}, \quad (26)$$

where, in turn,

$$\Phi_1(t) = \frac{1}{V\sqrt{2\pi}} e^{-t^2/2}, \quad \gamma = 1 - \frac{\hbar k_F}{M^* c} + \frac{1}{2} \left( \frac{\Omega}{M^* c^2} \right) x.$$

Before proceeding from  $P$  to the gamma-ray absorption cross section we shall determine the density of final levels. The density of states  $\Phi_b$  with energy  $E_\gamma$  is given by

$$\rho(E_\gamma) = dL(E_\gamma) / dE_\gamma,$$

where  $L(E_\gamma)$  is the number of states  $\Phi_b$  with  $\epsilon_b \leq E_\gamma$ . For the determination of  $L(E_\gamma)$  it is necessary to compute the number of phase cells contained in the phase volume of the nucleon and the holes corresponding to all states  $\Phi_b$  with  $\epsilon_b \leq E_\gamma$ . In this case, as is shown by a simple calculation,

$$\rho(E_\gamma) = \frac{3V^2}{8\pi^4} \left( \frac{2M^*}{\hbar^2} \right)^3 \Omega^2 x^2 \int_{\xi(x)}^{\sqrt{v(x)}} y^2 (1 + y^2)^{1/2} dy, \quad (27)$$

where

$$v(x) = \hbar^2 k_F^2 / 2M^* \Omega x,$$

$$\xi(x) = \begin{cases} \sqrt{v(x) - 1}, & v(x) > 1 \\ 0, & v(x) < 1 \end{cases}.$$

Before going from (25) to the cross section, (25) must be divided by the flux  $c/V$ . Then, using (27), we obtain

$$\sigma(E_\gamma) = 0.11 \cdot 10^{-26} A Z^2 F(x) \text{ cm}^2. \quad (28)$$

Here

$$F(x) = \left( \frac{M^*}{M} \right)^5 \varphi_2(x) \int_{\xi(x)}^{\sqrt{v(x)}} y^2 (1 + y^2)^{1/2} dy \left( \frac{\Omega}{1.1 \text{ Mev}} \right). \quad (29)$$

## 2. DISCUSSION OF RESULTS

In Fig. 1,  $F(x)$  is plotted for different values

\*The  $z$  axis is chosen to be in the direction  $Q$ .

†The  $x$  axis is in the direction of  $A_0$ .

of  $\Omega$  and  $M^*/M$ . In all cases the photonuclear absorption cross section given by (28) shows strong resonance, the frequency and width of which depend essentially on  $\Omega$ . In Ref. 7 a first estimate was obtained for  $W$ , which is related to  $\Omega$  by Eq. (12); the result was  $W \approx 23$  Mev ( $\Omega \approx 32$  Mev). Later and more accurate calculations gave  $W = 6 - 10$  Mev, which corresponds to  $\Omega = 8.4 - 14$  Mev. Because of this indefiniteness in the mag-

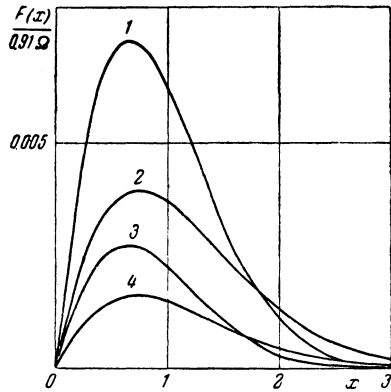


FIG. 1. 1— $\Omega = 10$ ,  $M^*/M = 1$ ; 2— $\Omega = 10$ ,  $M^*/M = 1/2$ ;  
3— $\Omega = 25$ ,  $M^*/M = 1$ ; 4— $\Omega = 25$ ,  $M^*/M = 1/2$ .

nitude of  $\Omega$ , in Fig. 1  $F(x)$  is given for two values of  $\Omega$  (10 Mev and 25 Mev). The magnitude of  $\Omega$  depends generally on  $E_\gamma$  and increases somewhat with  $E_\gamma$ . However, since the form of the function  $\Omega(E_\gamma)$  is unknown the curves in Fig. 1 were plotted with  $\Omega$  assumed to be constant. Even if the slight dependence of  $\Omega$  on  $E_\gamma$  were taken into account, the curves of  $F(x)$  would not be essentially changed. The question of the effective mass of a nucleon in a nucleus has been discussed widely in the literature (see Refs. 13 and 14, for example).

It has thus been shown that  $\frac{1}{2}M < M^* < M$ , where  $M$  is the mass of a free nucleon. The curves of  $F(x)$  for each value of  $\Omega$  were plotted for the two limiting values of the effective mass. Figure 1 shows that independently of the magnitude of  $\Omega$ , when the effective mass is reduced from  $M^* = M$  to  $M^* = M/2$  the cross section is reduced by one half at the peak while the half width increases by 20—30%. The resonance frequency and the width depend slightly on  $M^*$ , which is in disagreement with Ref. 15. For different values of  $\Omega$  these quantities change considerably. It is difficult to make a numerical comparison of the foregoing calculation with experimental findings, because for no single nucleus have the cross sections been measured for all processes that pass through the compound nucleus

stage as a result of excitation by gamma rays\* in the considered energy range ( $E_\gamma < 50$  Mev). The available experiments with medium and heavy nuclei (the only nuclei for which it is meaningful to compare theory and experiment) are not qualitatively in disagreement with the foregoing calculation. Thus the observed resonance frequencies for the  $(\gamma, n)$ ,  $(\gamma, 2n)$ ,  $(\gamma, p)$ , etc. reactions correspond to  $\Omega \sim 15$  Mev. For this value of  $\Omega$  the half width of the cross section curve is 17—28 Mev, as follows from Fig. 1, which exceeds the observed half width for  $(\gamma, n)$  by a factor of 2 to 3,<sup>17</sup> and for  $(\gamma, \gamma)$  and  $(\gamma, \gamma')$  by a factor of 1.5 to 2. This discrepancy of the half widths can be accounted for by the following considerations:

(a) The theoretical cross section for photonuclear absorption when  $E_\gamma$  is below the Bethe-Hurwitz characteristic level<sup>18</sup> ( $E_{B-H} \sim 4 - 6$  Mev for non-fissioning nuclei) appears too large, because in this energy range there occurs resonance scattering of gamma rays at particular levels which experiment<sup>16</sup> shows to be considerably below the result calculated above. This reduces the calculated photonuclear absorption half width by  $\approx 5$  Mev.

(b) The cross sections for  $(\gamma, x)$  reactions which pass through the compound nucleus stage are obtained by multiplying the cross section of (28) by the relative probability of the respective process.

Since the thresholds of these reactions ( $E_x$ ) lie above the Bethe-Hurwitz level by 2—3 Mev,

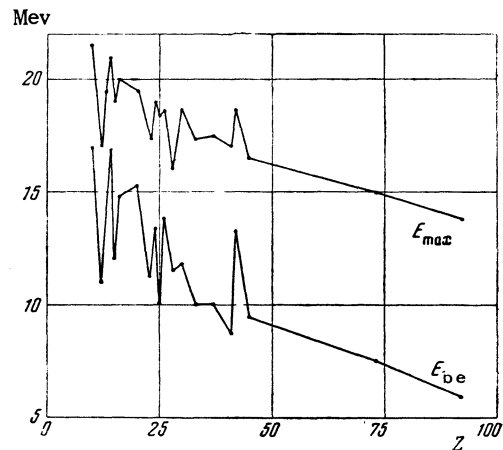


FIG. 2

the half width of the  $(\gamma, x)$  curve is less than that of the photoabsorption curve by 2—3 Mev and is thus 9—14 Mev. This is still greater than the

\*Thus, there is a complete absence of data on the  $(\gamma, \gamma')$  threshold below the  $(\gamma, n)$  threshold.

observed half width of 6–8 Kev. The agreement between theory and experiment is somewhat improved by taking into account the dependence  $\Omega(E_\gamma)$ , which follows from Eq. (26). When  $E_\gamma < E_x$  only the processes  $(\gamma, \gamma)$  and  $(\gamma, \gamma')$  can occur. However, the  $(\gamma, \gamma)$  cross sections in this energy range are small<sup>16</sup> compared with the calculated photoabsorption cross section, which apparently indicates that in this energy range considerable inelastic scattering of photons should be observed. Unfortunately, the requisite measurements are not yet available. Since, according to Ref. 7,  $\Omega$  depends slightly on atomic weight, the maximum and half width of the photonuclear absorption cross section should also depend slightly on  $A$ . Therefore, we should observe a correlation between the frequency at the  $(\gamma, n)$  cross section maximum and the binding energy of the emitted neutron (with increasing  $E_{be}$ ,  $E_{max}$  should increase and vice versa). The available experimental data actually reveal this tendency (Fig. 2).\*

The model of infinite nuclear matter which has been used cannot yield the observed relation between the cross section for gamma-ray capture and  $A$ . This is due principally to the fact that the level density which has been calculated above depends more strongly on the number of particles than the density of the corresponding levels in real nuclei. In addition, the same circumstance increases by more than one order of magnitude the maximum of the gamma-ray capture cross section. Thus for  $A = 100$ ,  $\sigma_\gamma(E_{max}) \approx 6$  barns, and for  $A = 200$ ,  $\sigma_\gamma(E_{max}) = 50$  barns. Better agreement between theory and experiment results from consideration of a finite nucleus.

In conclusion the authors wish to thank A. S.

Davydov and A. I. Leipunskii for their interest and for discussion of the results.

<sup>1</sup>A. B. Migdal, J. Exptl. Theoret. Phys. (U.S.S.R.) **15**, 81 (1945).

<sup>2</sup>M. Goldhaber and E. Teller, Phys. Rev. **74**, 1046 (1948).

<sup>3</sup>D. H. Wilkinson, Physica **22**, 1039 (1956).

<sup>4</sup>J. L. Burkhardt, Phys. Rev. **91**, 420 (1953).

<sup>5</sup>J. Fujita, Progr. Theoret. Phys. (Japan) **14**, 4, 400 (1955).

<sup>6</sup>Feshbach, Porter, and Weisskopf, Phys. Rev. **96**, 448 (1954).

<sup>7</sup>Lane, Thomas, and Wigner, Phys. Rev. **98**, 693 (1955).

<sup>8</sup>V. M. Agranovich and A. S. Davydov, J. Exptl. Theoret. Phys. (U.S.S.R.) **32**, 1429 (1957), Soviet Phys. JETP **5**, 1164 (1957).

<sup>9</sup>C. Bloch, Nucl. Phys. **3**, 137 (1957).

<sup>10</sup>L. Landau and E. Lifshitz, Квантовая механика (Quantum Mechanics), Vol. I, 1948.

<sup>11</sup>T. Teichmann and E. P. Wigner, Phys. Rev. **87**, 123 (1952).

<sup>12</sup>E. Vogt and Lascoux, CRT-679, Atomic Energy of Canada Ltd., Chalk River Project, Chalk River, Ont.

<sup>13</sup>H. A. Bethe and J. Goldstone, Proc. Roy. Soc. (London) **A238**, 551 (1956).

<sup>14</sup>W. Wada and K. A. Brueckner, Phys. Rev. **103**, 1008 (1956).

<sup>15</sup>V. F. Weisskopf, Nucl. Phys. **3**, 423 (1957).

<sup>16</sup>J. S. Levinger, Phys. Rev. **84**, 523 (1951).

<sup>17</sup>N. Kul'chitskii, Проблемы современной физики (Problems of Contemp. Phys.) No. 6, 5 (1957).

<sup>18</sup>H. A. Bethe and H. Hurwitz, Phys. Rev. **81**, 898 (1951).

<sup>19</sup>S. Rand, Phys. Rev. **107**, 208 (1957).

\*The experimental data were taken from the review article, Ref. 17.

Translated by I. Emin